Cell. Mol. Biol. (ISSN: 1165-158X)

Journal Homepage: www.cellmolbiol.org

Cellular and Molecular Biology

Original Article

Molecular evaluation of quercetin effects in a murine model of giant cell tumor of bone: an *in vivo* pilot study

Dalia Lizbeth Monroy-Quiroz [1,2#], Alexandra Berenice Luna-Angulo [3#], Brandon Eduardo Galicia-Canales [1], Laura Sánchez-Chapul [3], Olivia Hernández-González [4], María del Rocío Aguilar-Gaytán [1], Mónica Guadalupe Santamaría-Olmedo [5], Alberto Hidalgo-Bravo [5], Beatriz del Carmen Couder-García [6], Gabriel Lara-Hernández [7], Erendira Georgina Estrada-Villaseñor [8*], Carlos Landa-Solís [1,*]

[1] *Cellular Therapy and Regenerative Medicine Tissue Engineering Unit, Instituto Nacional de Rehabilitación Luis Guillermo Ibarra Ibarra, Mexico City 14389, Mexico*
[2] *Instituto Tecnológico y de Estudios Superiores de Monterrey, Mexico City 14380, Mexico*
[3] *Laboratory of Neuromuscular Diseases, Division of Clinical Neurosciences, Instituto Nacional de Rehabilitación Luis Guillermo Ibarra Ibarra, Mexico City 14389, Mexico*
[4] *Laboratorio de Microscopía Electrónica, Instituto Nacional de Rehabilitación Luis Guillermo Ibarra Ibarra, Mexico City 14389, Mexico*
[5] *Genetic Laboratory, Instituto Nacional de Rehabilitación Luis Guillermo Ibarra Ibarra, Mexico City 14389, Mexico*
[6] *SECIHTI-Centro de Investigación y Asistencia en Tecnología y Diseño del Estado de Jalisco, Subsede Sureste, Parque Científico Tecnológico de Yucatán, Tablaje Catastral 31264, Mérida 97302, México*
[7] *BioMaussan research and development unit, Mexico City 01210, Mexico*
[8] *Pathological Anatomy Service Instituto Nacional de Rehabilitación Luis Guillermo Ibarra Ibarra, Mexico City 14389, Mexico*

Article Info

Article history:

Received: March 28, 2025
Accepted: June 25, 2025
Published: July 31, 2025

Use your device to scan and read the article online

Abstract

Quercetin, a flavonoid derived from plant sources, has been extensively studied for its numerous biological properties, particularly its potential antitumor action against various malignant neoplasms. In our experience with a giant cell tumor of bone cell line (TIB-223), we demonstrated that quercetin has the ability to induce apoptosis via caspase-3. Therefore, this study aimed to evaluate molecular markers for apoptosis, necrosis, and cell proliferation in a murine model of giant cell tumor of bone, to determine whether the behavior reported for quercetin in 2D remains consistent in a 3D *in vivo* tumor model. Tumor constructs based on TIB-223 cells were implanted into athymic mice, and two weeks post-implantation, the mice were orally administered quercetin at a concentration of 100 mg/kg body weight once a day for two weeks. The control group received only 200 µL of the vehicle. Our results demonstrate the activation of two cell death pathways in the implanted tumors: apoptosis, via Caspase-8 to Caspase-3 activation, and necroptosis, via RIPK1. No significant effect on cell proliferation was observed, as PCNA expression remained unchanged. Our results suggest that quercetin may induce specific mechanisms of cell death without significantly altering cell proliferation in the tumor model induced in mice.

Keywords: Giant cell tumor of bone, Side effects, Alternative therapies, Quercetin, *In vivo* models.

1. Introduction

Giant cell tumor (GCT), although histologically benign, is considered one of the most common bone neoplasms. This type of tumor is characterized by locally aggressive behavior and primarily affects young adults, being most common in individuals between the ages of 20 and 40, according to current epidemiological reports. It mainly affects the tibia or femur in the metaphyseal or epiphyseal regions [1]. It has been reported that there is no difference in its aggressiveness between the lower and upper extremities [2]. On the other hand, GCT has been reported in the cervical spine in elderly patients [3]. Histologically, GCT is mainly composed of mononuclear ovoid-shaped cells and multinucleated giant cells, the latter being directly associated with bone resorption in the tumor microenvironment [1]. Molecular studies have identified that approximately 90% of these tumors present the G34W mutation in the gene encoding histone H3.3 [4, 5]. This mutation is found exclusively in the neoplastic stromal cells and is absent in the osteoclast precursors [5]

One of its main characteristics is its aggressive behavior [2]. It can be classified as unpredictable, as it may present features ranging from focal bone or cortical destruction,

* Corresponding author.
E-mail address: eren_strada71@hotmail.com (E.G. Estrada-Villaseñor); cls_73@hotmail.com (C. Landa-Solís).
# These authors contributed equally
Doi: http://dx.doi.org/10.14715/cmb/2025.71.7.15

invasion of the surrounding soft tissues of the primary tumor [1], and metastasis, which is reported as infrequent [5], occurring in 2-9% of patients [6-8], and typically in the lungs in less than 8% of the studied patients [9].

The current standard treatment for GCT combines surgical interventions (curettage or resection) with medical therapy based on denosumab, which is the main therapeutic alternative available [10]. In cases of advanced GCT, it has been reported that 73% of patients require a surgical intervention with extensive resection and the use of endoprostheses to replace the resected bone tissue [9], resulting in dysfunction in patients' quality of life due to the loss of motor ability [11]. Additionally, side effects of current GCT treatments have been described: loss of tissue surrounding the tumor area due to necrosis induction [12, 13], damage to the neural pathways of the affected extremity [14], and the possibility of tumor recurrence after discontinuing denosumab treatment in 48% of patients after 24 months of monotherapy [15]. Furthermore, when denosumab is administered prior to surgical resection of the tumor, the recurrence risk is between 15% and 20% within 18 months [16].

Considering that the available therapeutic options for GCT treatment still have limitations in terms of efficacy and safety, our research group has focused on studying quercetin, a flavonoid with proven antitumor activity in various preclinical models [17-19], with the aim of evaluating the effect of quercetin as a potential therapeutic alternative for this neoplasm. Our in vitro results indicate that quercetin induces cell death through apoptosis via caspase-3 activation in a GCT cell line (TIB-223) [20]. In this study, we conducted a pilot in vivo study using a murine GCT model to evaluate molecular markers for apoptosis, necrosis, and cell proliferation, and to determine whether quercetin maintains the same behavior when transferred from a 2D in vitro model to a 3D in vivo model.

2. Materials and methods

2.1. Murine GCT model

The treatment was performed in accordance with the guidelines for the care and use of laboratory animals (NIH Publications No. 8023, revised in 1978) and was approved by the bioethics committee of the CEI-111-ORD-2019 Institute, as well as the Internal Committee for the Care and Use of Laboratory Animals (CICUAL/005/2019, identification number: 52/19). Six male CD1 athymic mice, weighing 30 g, heterozygous nu/nu, aged 9 months, were used. The mice were divided into two groups: Group 1 (3 control mice that were administered only the vehicle) and Group 2 (3 mice that were administered quercetin). The mice were provided with water and standard maintenance food ad libitum, previously sterilized, in cages connected to an animal rack with HEPA-filtered air at low speed, with a 12-hour light/dark cycle, an average temperature of 25°C, and 50% humidity.

2.2. Construct preparation

The construct was prepared using the TIB-223 cell line, which has been described and used in *in vitro* models of Giant Cell Tumor of Bone [21, 22]. The cells were expanded in cell culture (McCoy's 5A medium, 10% fetal bovine serum, and 1% antibiotic-antimycotic, Gibco, Life Technologies, Carlsbad, CA, USA) until a sufficient number of cells for the experiments was obtained. The cells were then frozen in cryovials at a concentration of $1x10^6$/mL and stored in liquid nitrogen until use.

2.3. Three-dimensional (3D) scaffold printing

The design of the 3D-printed tumor model was carried out according to the method described by Estrada et al. [23]. A polycaprolactone (PCL) pellet was used as the raw material. The printing conditions were as follows: pore size of 850 µm, filament thickness of 200 µm, printing angle of 90°, with a total of 7 layers and no solid base, to form a 5 mm^3 cube (a REGEMAT 3D bio-printer, designed at the University of Granada, Spain, was used). Once the scaffolds were printed, they were sterilized using the ethylene oxide method [24]. Then, under sterile conditions within the laminar flow hood, $2x10^6$ TIB-223 cells were seeded onto each scaffold (Figure 1A), as previously described by Landa et al. [25]. The constructs (scaffolds with seeded cells) were maintained under culture conditions (37°C with a 5% CO_2 atmosphere, McCoy's 5A medium, 10% fetal bovine serum, and 1% antibiotic-antimycotic, Gibco, Life Technologies, Carlsbad, CA, USA) for 4 days to achieve consolidation of the constructs before implantation (Figure 1B).

2.4. Implantation of the construct

The construct implantation was carried out in the animal handling facilities, specifically in the immunocompromised animal handling area (throughout the experimental process). Within the laminar flow hood, general anesthesia was administered by inhalation using 4% isoflurane. The implantation was performed in the dorsal-thoracic area (after antisepsis), making an incision of 1 cm that extended to the subcutaneous tissue. Using fine-tipped forceps, the tissue was separated until the necessary space was obtained to house the construct. To prevent displacement of the construct from the implantation area, a 3-0 nylon suture was used to anchor the construct to the adjacent muscle. Finally, the incision was closed with two "U" sutures in a single plane (Figures 1D and 1E). The mice, before receiving the treatment, were housed in separate cages by group for two weeks and were provided with water and food.

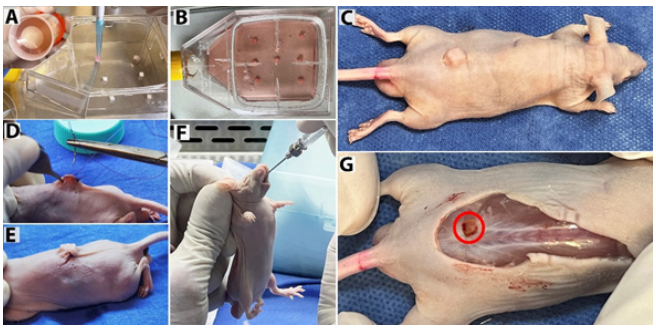

Fig. 1. Experimental design. (A) TIB-223 cells, previously expanded in cell culture, were seeded at 2x106 cells on a 3D-printed scaffold made of polycaprolactone. (B) Consolidation of the tumor constructs (scaffolds with TIB-223 cells), which were maintained in culture for 4 days. (D and E) The constructs were implanted in the dorsal-thoracic region of the athymic mice and were kept isolated for two weeks before starting treatment. (F) Administration of the treatment using stainless steel gastric applicators. (C and G) After treatment, the mice were euthanized, and the tumor constructs were dissected (marked with a red circle), and stored at -80°C for molecular analysis.

2.5. Treatment of the murine GCT model

The treatment of the mice was administered orally using curved stainless steel gastric applicators with a blunt tip, 44 mm long and 0.78 mm in diameter, previously sterilized by steam under pressure (15 psi, 121°C, for 15 minutes). The treated group received 100 mg/kg of quercetin (Sigma-Aldrich, Darmstadt, Germany) [26, 27], diluted in 200 µL of the vehicle (highly refined, low acidity olive oil, Sigma-Aldrich, Darmstadt, Germany), once every 24 hours for 14 days, while the control group received 200 µL of the vehicle (Figure 1F). After the treatment administration, the mice were euthanized (Figure 1C), and the tumor constructs were dissected, keeping them free of soft tissues (Figure 1G), and all collected tissue was immediately stored at -80°C for subsequent molecular analysis.

2.6. Western blot analysis

Tumor fragments obtained from the treated mice (quercetin 100 mg/kg body weight) and the control group (vehicle 200 µL olive oil), approximately 30 mg, were used for the detection of pro-caspase 3 and caspase 3 with the primary antibody anti-caspase-3 (SC-56053, Santa Cruz Biotechnology, TX, USA). The tumor fragments were placed in 15 mL Falcon tubes (previously washed with 1X PBS), 300 µL of RIPA lysis buffer (Santa Cruz Biotechnology, TX, USA) was added, the samples were sonicated, and incubated at 4°C for 30 minutes. Then, the samples were centrifuged for 20 minutes at 15,000 rpm at 4°C. To separate the proteins by electrophoresis (previously quantified to 60 µg), a 12% SDS-PAGE gel was used. The proteins were transferred to a nitrocellulose membrane, and non-specific binding sites were blocked using 5% skim milk in Tris-buffered saline with Tween 20 (TBST) (NaCl 150 mM, Tris-HCl 10 mM (pH 7.4), and 0.1% Tween-20). The membrane was incubated overnight at 4°C with the primary antibody. A secondary antibody was used: anti-rabbit IgG conjugated with horseradish peroxidase (Bio-Rad, Hercules, CA, USA), and incubated for 1 hour at room temperature. The chemiluminescence detection reagent (Millipore, Burlington, MA, USA) was added, and the membrane was washed with PBS. For image digitization, the C-DiGit® Blot Scanner (LI-COR Biosciences, NE, USA) was used, and for band density quantification, the Image Studio Digits V4.0 program (LI-COR Biosciences, NE, USA) was employed. For the positive control of caspase-3 expression, 1x106 TIB-223 cells from a monolayer culture were exposed to a standardized dose of H2O2 (125 µM) for 3 hours, and then the procedure was performed as described above [28].

2.7. qPCR analysis

Total RNA was extracted from the tissues obtained from both treated and untreated mice using Trizol (Invitrogen, Carlsbad, California, USA) [29]. From 1 µg of total RNA, cDNA was synthesized using the QuantiTect® Reverse Transcription Kit (Qiagen, Hilden, Germany). For real-time quantification (RT-PCR), the SYBR Green Premix Kit (Bio-Rad, Hercules, California, USA) was used. The primer sequences employed are listed in Table 1. Relative mRNA quantification was performed using the delta-delta CT (ΔΔCT) method.

2.8. Statistical analysis

The data obtained from the quantification of Western blot bands and real-time qPCR for both the treated and control groups are presented as mean ± standard deviation. Statistical analysis was performed using GraphPad Prism version 9. An unpaired t-test was used to compare the groups, and statistically significant differences were defined as $p < 0.05$.

3. Results

3.1. Western blot analysis

Western blot analysis was performed on tumor fragments from mice treated with quercetin (100 mg/kg) and control mice treated with vehicle (200 µL olive oil). The expression of pro-caspase-3 (32 kDa) and its activated forms (caspase-3, 11, 17, and 20 kDa) was evaluated using a specific anti-caspase-3 antibody. The gel revealed a reduction in the intensity of the band corresponding to pro-caspase-3 in tumor samples from quercetin-treated mice compared to the control group, while the bands corresponding to the activated forms—particularly the 17 kDa band (caspase-3 p17)—showed increased intensity in the treated group. This suggests enhanced caspase-3 activation induced by quercetin (Figure 2A).

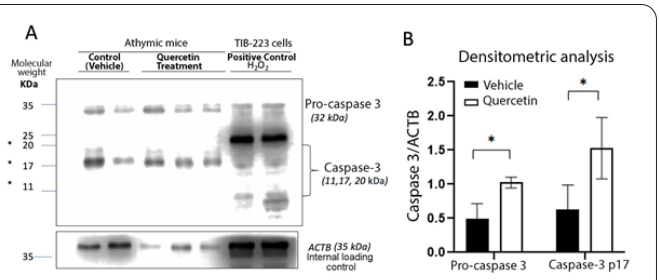

Fig. 2. Expression and activation of caspase-3 in giant cell tumors implanted in mice. (A)Western blot analysis of pro-caspase-3 (32 kDa) and its activated forms (caspase-3, 11, 17, and 20 kDa) in tumor fragments from mice treated with quercetin and those that received only vehicle. As a positive control, TIB-223 cells treated with hydrogen peroxide (H_2O_2) were used, showing robust caspase-3 activation. ACTB protein (35 kDa) was used as a loading control. (B) Densitometric analysis of the bands corresponding to pro-caspase-3 and caspase-3 p17, normalized to ACTB. Data are presented as mean ± SD; asterisks (*) indicate statistically significant differences ($p < 0.05$).

Table 1. Primer Sequences.

Gene	Forward	Reverse
HPRL27	CTGGGAAGGTGGTGCTTGTC	TAGCGGTCAATTCCAGCCAC
Caspasa 3	AGAGGGGATCGTTGTAGAAGTC	ACAGTCCAGTTCTGTACCACG
Caspasa 8	ATTTGCCTGTATGCCCGAGC	CCTGAGTGAGTCTGATCCACAC
RIP	TGGGCGTCATCATAGAGGAAG	CGCCTTTTCCATGTAAGTAGCA
PCNA	CCTGCTGGGATATTAGCTCCA	CAGCGGTAGGTGTCGAAGC

For the amplification of target genes by RT-qPCR. Forward and reverse sequences are listed for each gene, including HPRL27 (housekeeping gene), Caspase 3, Caspase 8, RIP, and PCNA.

Additionally, a positive control using TIB-223 cells treated with H_2O_2 confirmed robust expression of the activated forms of caspase-3. Densitometric analysis of the bands, normalized to ACTB, showed that pro-caspase-3 expression was significantly lower in the quercetin-treated group compared to the control group ($p = 0.023$). Although the expression of caspase-3 p17 was higher in the treated group, the difference did not reach statistical significance ($p = 0.058$) (Figure 2B). These data demonstrate that quercetin treatment induces changes in caspase-3 proteolysis, consistent with apoptosis induction in the evaluated tumor model, further supported by the positive control with H_2O_2-treated TIB-223 cells.

3.2. qPCR analysis of GCT

Following real-time qPCR analysis of tumor fragments extracted from treated and control mice, significant changes were observed in the expression of genes associated with apoptosis, necrosis, and cell proliferation after quercetin treatment. For Caspase 8, a marked increase was observed in the treated group (~250 relative units) compared to the control group (~50 units), with a statistically significant difference ($p = 0.032$), suggesting activation of the extrinsic apoptotic pathway (Figure 3A). In contrast, Caspase 3 expression showed a slight decrease in treated mice (0.8 U vs. 1.1 U in the control group), though without statistical significance ($p = 0.13$) (Figure 3B). The RIPK1 gene, associated with regulated necrosis, exhibited a dramatic increase in the quercetin group (~1400 U) compared to the control (~100 U), with a highly significant difference ($p = 0.01$) (Figure 3C), indicating a possible activation of non-apoptotic cell death in addition to that induced by the extrinsic apoptosis pathway. Finally, PCNA expression, a marker of cell proliferation, showed a slight increase in the treated group (~2.5 U vs. 2 U in the control group), without reaching statistical significance ($p = 0.66$) (Figure 3D), ruling out a direct effect of quercetin on cell proliferation as a result of treatment. Quercetin induced a significant increase in Caspase 8 and RIPK1, suggesting activation of both apoptosis and necrosis in the treated group.

4. Discussion

As reported in our previous study, where TCG cells (TIB-223) were exposed to quercetin in vitro for 24 hours at two concentrations of 91.1 µM, the cell population was predominantly positive for apoptosis (84.48%), with a smaller fraction positive for necrosis (3.14%), and a third population expressing both markers (11.84%), considered indicative of necroptosis. Protein analysis demonstrated that apoptosis was induced through caspase-3 activation [20]. In the present study, we advanced this approach by applying it in a murine model of giant cell tumor, using a dose of 100 mg/kg body weight for two weeks in athymic mice—a dose previously used in other in vivo tumor models with favorable outcomes [26, 27]. This study shows that quercetin exerts an antitumor effect through the simultaneous activation of multiple cell death pathways.

Western blot analysis of protein expression revealed that the treated group exhibited reduced intensity of the bands corresponding to pro-caspase-3 compared to the control group. In contrast, the bands corresponding to the activated forms, particularly the 17 kDa band (caspase-3 p17), showed a trend toward increased intensity, suggesting that the apoptotic pathway was mediated by caspase-3 activation. On the other hand, RT-qPCR analysis of caspase-3 expression did not show statistically significant differences in mRNA levels between the groups. Therefore, we propose that the discrepancy between mRNA levels and protein expression suggests that caspase-3 activation is more dependent on post-translational mechanisms than on transcriptional regulation of the gene, as has been reported in other experimental models where a dissociation between caspase-3 mRNA and protein expression has been observed [30-32].

Notably, unlike caspase-3, the analysis of caspase-8 expression showed a significant increase compared to the control group ($p = 0.032$), suggesting possible activation of the extrinsic apoptosis pathway mediated by death receptors, as has been reported in the BT-474 breast cancer cell line [33], and in the HL-60 acute leukemia cell line, where quercetin was found to regulate pro-apoptotic and anti-apoptotic proteins such as Bax and Bcl-2 [34].

Another cell death pathway identified through RIPK1 gene overexpression was necroptosis. RIPK1 expression showed a significant increase in the treated group compared to the control ($p = 0.01$). The activation of this pathway by quercetin is of great relevance, as it broadens the range of therapeutic options for tumors resistant to classical apoptotic mechanisms, such as diffuse large B-cell lym-

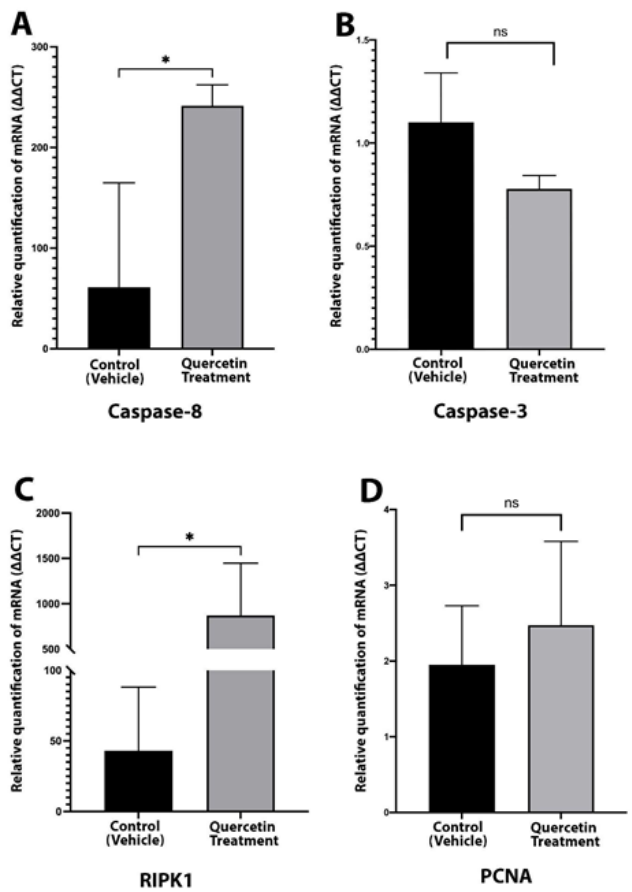

Fig. 3. Graphical representation of RT-qPCR gene expression analysis in tissue from quercetin-treated mice vs. control group. The mRNA levels were evaluated for: (A) Caspase 8 expression ($p = 0.032$), (B) Caspase 3 expression ($p = 0.13$), (C) RIPK1, a necrosis marker, and (D) PCNA expression ($p = 0.66$). Data are presented as mean ± standard deviation (SD) of relative quantification ($2^{-\Delta\Delta CT}$). Asterisks (*) indicate statistically significant differences ($p < 0.05$), and "ns" indicates no significant difference.

phoma [35]. Additionally, the activation of this alternative mechanism of cell death by quercetin has also been reported in isolated cholangiocarcinoma cells through activation of the RIPK1/RIPK3/MLKL pathway [36], supporting our findings in the induced GCT model.

Finally, an interesting finding in the induced murine GCT model was the absence of significant changes in the expression of PCNA, a marker of cell proliferation ($p = 0.66$). Based on this result, we suggest that quercetin does not promote tumor cell proliferation, which is consistent with the antiproliferative effect previously described in our in vitro study [20].

The main limitations of this work include its pilot study nature, involving a small sample size and a limited number of molecular markers evaluated. Nonetheless, our findings suggest that quercetin possesses antitumor potential against GCT through a dual mechanism, inducing both apoptosis and necroptosis. This mechanism could be particularly valuable for tumors resistant to conventional treatments. Our evidence provides a foundation for further research into the molecular mechanisms involved and supports the use of electron microscopy to verify apoptosis and necrosis in the in vivo murine model over the long term, potentially paving the way for the design of clinical study protocols.

This pilot study provided a preliminary overview of the various cell death pathways activated by quercetin in a murine model of GCT, identifying two main mechanisms of action: apoptosis and necroptosis. The therapeutic potential of quercetin for the treatment of GCT, without the side effects associated with current therapies, highlights its capacity to improve the quality of life for patients with GCT.

Acknowledgments
We thank Ingrid Salgado Gutiérrez, Aarón Ernesto Marure-Rojano, and José Ricardo Cano-García for their help in preparing the material required for the development of the study, and all staff responsible for the institute's animal handling facilities.

Conflict of interests
The author has no conflicts with any step of the article preparation.

Consent for publications
The author read and approved the final manuscript for publication.

Ethics approval and consent to participate
The present research was approved by the bioethics committee of the CEI-111-ORD-2019 Institute, as well as the Internal Committee for the Care and Use of Laboratory Animals (CICUAL/005/2019, identification number: 52/19).

Informed consent
The authors declare that no patients were used in this study.

Availability of data and material
The data that support the findings of this study are available from the corresponding author upon reasonable request.

Authors' contributions
Conceptualization, C.L.-S; methodology, D.L.M.-Q., B.E.G.-C., and M.d.R.A.-G.; validation, L.S.-C., M.G.S.-O., O.H.-G., A.B.L.-A., and M.d.R.A.-G.; formal analysis, O.H.-G. and E.G.E.-V.; investigation, D.L.M.-Q., M.G.S.-O., L.S.-C., E.G.E.-V., and B.E.G.-C.; resources, M.G.S.-O., O.H.-G., B.d.C.C.-G., and E.G.E.-V.; data curation, C.L.-S., and G.L.-H., writing original draft preparation, C.L.-S., D.L.M.-Q., B.E.G.-C., and A.B.L.-A.; writing review and editing, C.L.-S and G.L.-H.; visualization, M.d.R.A.-G., B.d.C.C.-G., and A.H.-B.; Quality control of raw materials, B.d.C.C.-G., G.L.-H., and A.H.-B., supervision, C.L.-S., M.G.S.-O., A.B.L.-A., and A.H.-B.; project administration, C.L.-S.; funding acquisition, C.L.-S. All authors have read and agreed to the published version of the manuscript.

Funding
None

References

1. Zuo D, Zheng L, Sun W, Fu D, Hua Y, Cai Z (2013) Contemporary adjuvant polymethyl methacrylate cementation optimally limits recurrence in primary giant cell tumor of bone patients compared to bone grafting: a systematic review and meta-analysis. World J Surg Oncol 11:156. doi: 10.1186/1477-7819-11-156
2. Saputra RD, Kusuma DA, Kaldani F, Fahmi K (2025) Comparative analysis of aggressiveness in giant cell tumor of bone between upper and lower extremities: A systematic review and meta-analysis. J Bone Oncol 51:100663. doi: 10.1016/j.jbo.2025.100663
3. Alolayan OA, Korkoman AJ, Alnasser AA (2025) Giant cell tumor of the cervical spine: A case report. Int J Surg Case Rep 126:110676. doi: 10.1016/j.ijscr.2024.110676
4. Papke DJ, Jr., Kovacs SK, Odintsov I, Hornick JL, Raskin KA, Newman ET, Lozano-Calderón S, Chebib I, Hung YP, Nielsen GP (2025) Malignant Giant Cell Tumor of Bone: A Clinicopathologic Series of 28 Cases Highlighting Genetic Differences Compared With Conventional, Atypical, and Metastasizing Conventional Tumors. Am J Surg Pathol 49:539-553. doi: 10.1097/pas.0000000000002387
5. Yao Y, Lee VKM, Chen ES (2025) Molecular pathological insights into tumorigenesis and progression of giant cell tumor of bone. J Bone Oncol 51:100665. doi: 10.1016/j.jbo.2025.100665
6. Balke M, Schremper L, Gebert C, Ahrens H, Streitbuerger A, Koehler G, Hardes J, Gosheger G (2008) Giant cell tumor of bone: treatment and outcome of 214 cases. J Cancer Res Clin Oncol 134:969-978. doi: 10.1007/s00432-008-0370-x
7. Errani C, Ruggieri P, Asenzio MA, Toscano A, Colangeli S, Rimondi E, Rossi G, Longhi A, Mercuri M (2010) Giant cell tumor of the extremity: A review of 349 cases from a single institution. Cancer Treat Rev 36:1-7. doi: 10.1016/j.ctrv.2009.09.002
8. Sanjay BK, Kadhi SM (1998) Giant cell tumour of bone with pulmonary metastases. A report of three cases. Int Orthop 22:200-204. doi: 10.1007/s002640050242
9. do Couto FB, Yonamine ES, Magno FG, Favacho-Silva AB, de Brito CRA, Brito TRB (2025) Treatment of patients with giant cell bone tumor in northern Brazil, in 2020 and 2021. Acta Ortop Bras 33:e285342. doi: 10.1590/1413-785220253301e285342
10. Fellows D, Kotowska J, Stevenson T, Brown J, Orosz Z, Siddiqi A, Whitwell D, Cosker T, CLMH GI (2025) Management and surveillance of metastatic giant cell tumour of bone. Pathol Oncol Res 31:1611916. doi: 10.3389/pore.2025.1611916
11. Jain A, Aggrawal A, Sahu A, Agarwal R, Tiwari A (2024) Management of Giant Cell Tumor of Distal Radius-Does Curettage

Work? Indian J Surg Oncol 15:578-583. doi: 10.1007/s13193-024-01952-8

12. Emori M, Hamada K, Omori S, Joyama S, Tomita Y, Hashimoto N, Takami H, Naka N, Yoshikawa H, Araki N (2012) Surgery with vascular reconstruction for soft-tissue sarcomas in the inguinal region: oncologic and functional outcomes. Ann Vasc Surg 26:693-699. doi: 10.1016/j.avsg.2011.12.003
13. Emori M, Kaya M, Sasaki M, Wada T, Yamaguchi T, Yamashita T (2012) Pre-operative selective arterial embolization as a neoadjuvant therapy for proximal humerus giant cell tumor of bone: radiological and histological evaluation. Jpn J Clin Oncol 42:851-855. doi: 10.1093/jjco/hys090
14. Domovitov SV, Chandhanayingyong C, Boland PJ, McKeown DG, Healey JH (2016) Conservative surgery in the treatment of giant cell tumor of the sacrum: 35 years' experience. J Neurosurg Spine 24:228-240. doi: 10.3171/2015.4.Spine13215
15. Oran B, Garcia-Manero G, Saliba RM, Alfayez M, Al-Atrash G, Ciurea SO, Jabbour EJ, Mehta RS, Popat UR, Ravandi F, Alousi AM, Kadia TM, Konopleva M, DiNardo CD, Rezvani K, Shpall EJ, Sharma P, Kantarjian HM, Champlin RE, Daver N (2020) Posttransplantation cyclophosphamide improves transplantation outcomes in patients with AML/MDS who are treated with checkpoint inhibitors. Cancer 126:2193-2205. doi: 10.1002/cncr.32796
16. Scoccianti G, Totti F, Scorianz M, Baldi G, Roselli G, Beltrami G, Franchi A, Capanna R, Campanacci DA (2018) Preoperative Denosumab With Curettage and Cryotherapy in Giant Cell Tumor of Bone: Is There an Increased Risk of Local Recurrence? Clin Orthop Relat Res 476:1783-1790. doi: 10.1007/s11999.0000000000000104
17. Hoinoiu T, Dumitrascu V, Pit D, Schipor DA, Jabri-Tabrizi M, Hoinoiu B, Petreuș DE, Seiman C (2025) Quercetin as a Potential Therapeutic Agent for Malignant Melanoma-A Review of Current Evidence and Future Directions. Medicina (Kaunas) 61. doi: 10.3390/medicina61040656
18. Zhan XZ, Wei TH, Huang C, Yu H, Chen XL, Kong XT, Shang ZH, Sun SL, Lu MY, Ni HW (2025) Modulating JAK2/STAT3 signaling by quercetin in Qiling Baitouweng Tang: a potential therapeutic approach for diffuse large B-cell lymphoma. Mol Divers 29:2407-2431. doi: 10.1007/s11030-024-10999-2
19. Zhang J, Guo J, Qian Y, Yu L, Ma J, Gu B, Tang W, Li Y, Li H, Wu W (2025) Quercetin Induces Apoptosis Through Downregulating P4HA2 and Inhibiting the PI3K/Akt/mTOR Axis in Hepatocellular Carcinoma Cells: An In Vitro Study. Cancer Rep (Hoboken) 8:e70220. doi: 10.1002/cnr2.70220
20. Marure-Rojano AE, Cano-García JR, Luna-Agulo AB, Sánchez-Chapul L, Santos-Cuevas CL, Aguilar-Gaytán MDR, Flores-Berrios EP, Couder-García BDC, Lara-Hernández G, Bahena-Ocampo IU, Landa-Solís C (2025) The cytotoxic effect of quercetin-induced apoptosis on lung metastatic cells from giant cell tumor of bone. Cell Mol Biol (Noisy-le-grand) 71:6-12. doi: 10.14715/cmb/2025.71.5.2
21. Lara-Hernández G, Ramos-Silva JA, Pérez-Soto E, Figueroa M, Flores-Berrios EP, Sánchez-Chapul L, Andrade-Cabrera JL, Luna-Angulo A, Landa-Solís C, Avilés-Arnaut H (2024) Anticancer Activity of Plant Tocotrienols, Fucoxanthin, Fucoidan, and Polyphenols in Dietary Supplements. Nutrients 16. doi: 10.3390/nu16244274
22. Moore C, Fernandes RJ, Manrique J, Polissar NL, Miljacic L, Hippe DS, Vaux J, Thompson MJ (2022) Cytotoxic Effects of Common Irrigation Solutions on Chondrosarcoma and Giant Cell Tumors of Bone. J Bone Joint Surg Am 104:2153-2159. doi: 10.2106/jbjs.22.00404
23. Estrada-Villaseñor E, Valdés-Flores M, Meneses-García A, Silva-Bermudez P, Pichardo-Bahena R, Ostoa-Saloma P, Mercado-Celis G, Delgado-Cedillo ED, Olivos-Meza A, Landa-Solís C (2021) A novel model to culture cells from giant cell tumor of bone using three-dimensional (3D) polycaprolactone scaffold. Eng Life Sci 21:539-543. doi: 10.1002/elsc.202100020
24. Ghobeira R, Philips C, Declercq H, Cools P, De Geyter N, Cornelissen R, Morent R (2017) Effects of different sterilization methods on the physico-chemical and bioresponsive properties of plasma-treated polycaprolactone films. Biomed Mater 12:015017. doi: 10.1088/1748-605X/aa51d5
25. Landa-Solís C, Ibarra C, Salinas-Rojas A, Ortega-Sánchez C, Luna-Angulo AB, Aguilar-Gaytán MdR, Hazan-Lasri EJ (2023) An Osteocartilaginous 3D Printing Implant Using a Biocompatible Polymer and Pre-Differentiated Mesenchymal Stem Cells in Sheep. Applied Sciences 13:10177. doi:
26. Hashemzaei M, Delarami Far A, Yari A, Heravi RE, Tabrizian K, Taghdisi SM, Sadegh SE, Tsarouhas K, Kouretas D, Tzanakakis G, Nikitovic D, Anisimov NY, Spandidos DA, Tsatsakis AM, Rezaee R (2017) Anticancer and apoptosis-inducing effects of quercetin in vitro and in vivo. Oncol Rep 38:819-828. doi: 10.3892/or.2017.5766
27. Yang H, Yang T, Heng C, Zhou Y, Jiang Z, Qian X, Du L, Mao S, Yin X, Lu Q (2019) Quercetin improves nonalcoholic fatty liver by ameliorating inflammation, oxidative stress, and lipid metabolism in db/db mice. Phytother Res 33:3140-3152. doi: 10.1002/ptr.6486
28. Singh M, Sharma H, Singh N (2007) Hydrogen peroxide induces apoptosis in HeLa cells through mitochondrial pathway. Mitochondrion 7:367-373. doi: 10.1016/j.mito.2007.07.003
29. Zhang F, Wang ZM, Liu HY, Bai Y, Wei S, Li Y, Wang M, Chen J, Zhou QH (2010) Application of RT-PCR in formalin-fixed and paraffin-embedded lung cancer tissues. Acta Pharmacol Sin 31:111-117. doi: 10.1038/aps.2009.178
30. Fitzgerald JC, Ufer C, De Girolamo LA, Kuhn H, Billett EE (2007) Monoamine oxidase-A modulates apoptotic cell death induced by staurosporine in human neuroblastoma cells. J Neurochem 103:2189-2199. doi: 10.1111/j.1471-4159.2007.04921.x
31. Gor R, Gharib A, Dharshini Balaji P, Madhavan T, Ramalingam S (2023) Inducing Cytotoxicity in Colon Cancer Cells and Suppressing Cancer Stem Cells by Dolasetron and Ketoprofen through Inhibition of RNA Binding Protein PUM1. Toxics 11. doi: 10.3390/toxics11080669
32. Steinman RA, Johnson DE (2000) p21WAF1 prevents down-modulation of the apoptotic inhibitor protein c-IAP1 and inhibits leukemic apoptosis. Mol Med 6:736-749. doi:
33. Seo HS, Ku JM, Choi HS, Choi YK, Woo JK, Kim M, Kim I, Na CH, Hur H, Jang BH, Shin YC, Ko SG (2016) Quercetin induces caspase-dependent extrinsic apoptosis through inhibition of signal transducer and activator of transcription 3 signaling in HER2-overexpressing BT-474 breast cancer cells. Oncol Rep 36:31-42. doi: 10.3892/or.2016.4786
34. Niu G, Yin S, Xie S, Li Y, Nie D, Ma L, Wang X, Wu Y (2011) Quercetin induces apoptosis by activating caspase-3 and regulating Bcl-2 and cyclooxygenase-2 pathways in human HL-60 cells. Acta Biochim Biophys Sin (Shanghai) 43:30-37. doi: 10.1093/abbs/gmq107
35. Gourisankar S, Krokhotin A, Ji W, Liu X, Chang CY, Kim SH, Li Z, Wenderski W, Simanauskaite JM, Yang H, Vogel H, Zhang T, Green MR, Gray NS, Crabtree GR (2023) Rewiring cancer drivers to activate apoptosis. Nature 620:417-425. doi: 10.1038/s41586-023-06348-2